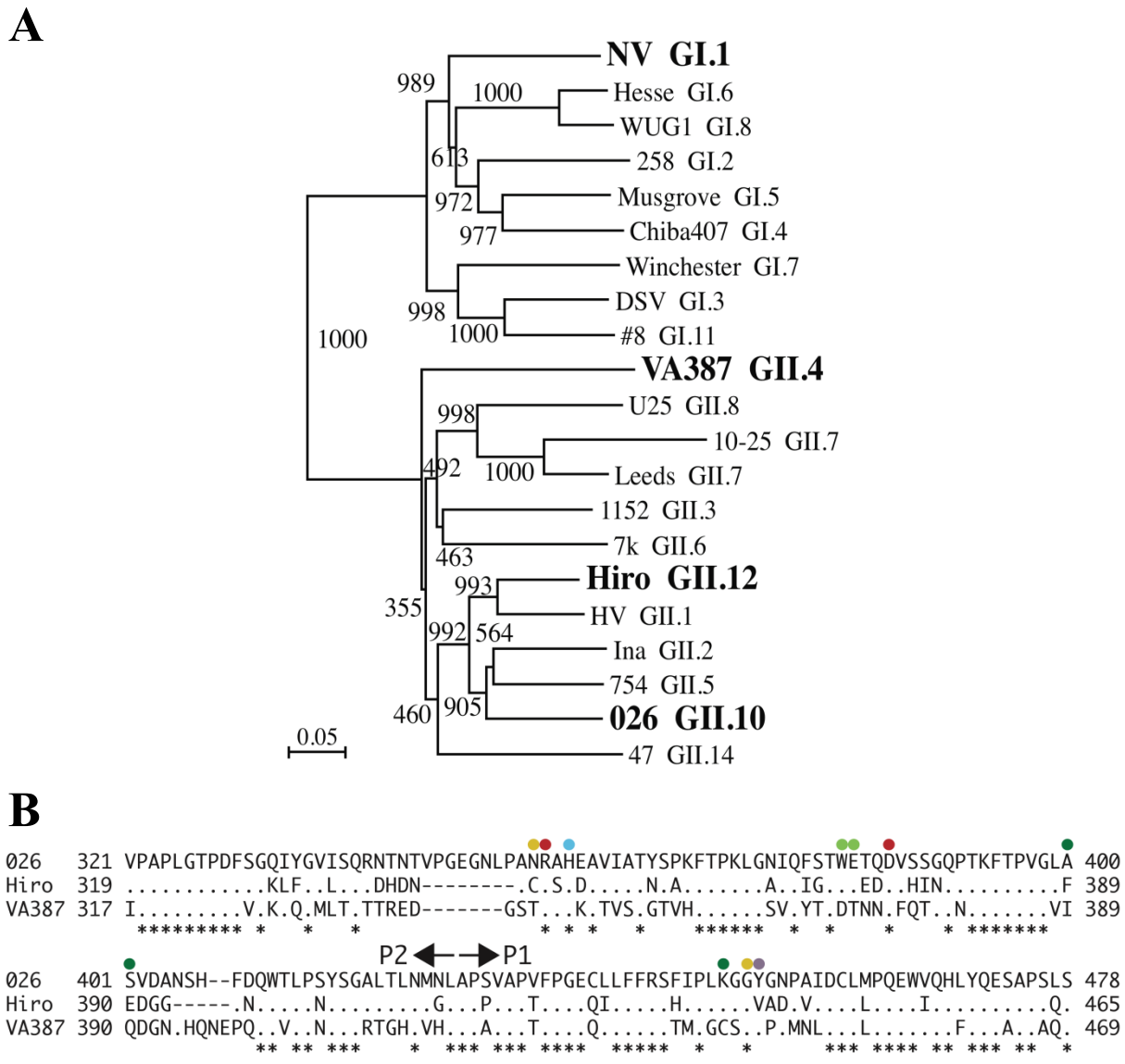

Figure S1. Phylogenic tree of GI and GII norovirus full-length amino acid capsid sequences and partial sequence alignment of Vietnam026, Hiro, and VA387. Noroviruses are genetically and antigenically diverse, though the majority of outbreak strains belong to GII.4. (A) The numbers on the branches indicate the bootstrap values for the clusters. Including this study, four norovirus P domains structures bound with different HBGAs have been determined GII.4, GI.1, GII.10, and GII.12. The 026 capsid had 78, 63, and 47% amino acid identity with Hiro, VA387, and NV, respectively, whereas Hiro had 66 and 47% amino acid identity with VA387 and NV, respectively. (B) Partial sequence alignment of three GII P domains showing the GII.10 P1 and P2 subdomain residues involved directly or indirectly with HBGAs (colored circles), where red (side-chain interactions with αfucose1-2), orange (backbone interactions with αfucose1-2), purple (hydrophobic interactions with αfucose1-2), light green (side-chain non-αfucose1-2 interactions), and dark green (backbone non-αfucose1-2 interactions). The asterisks show conserved residues and the arrows show the P1 and P2 subdomains.

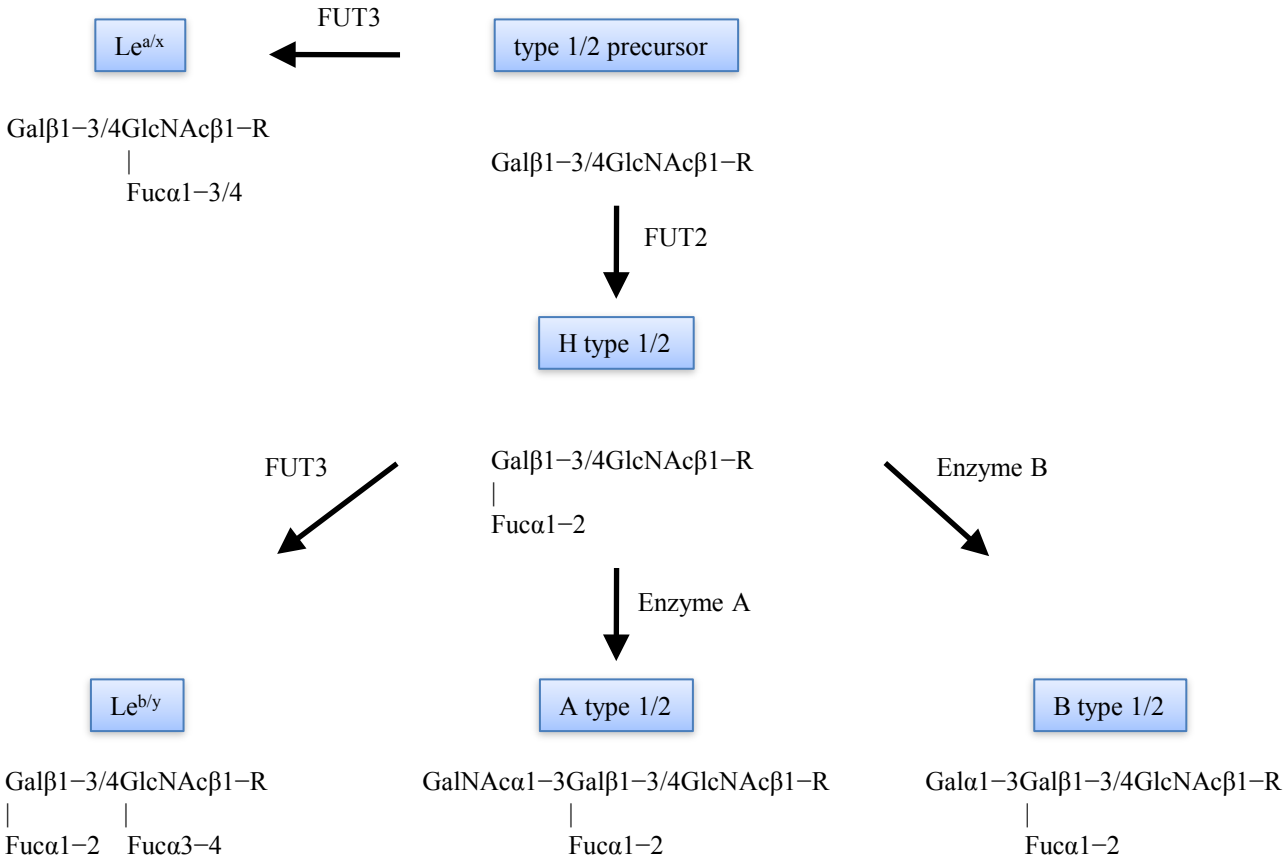

Figure S2. One of the major HBGA biosynthesis pathways, starting from the precursor type 1/2. HBGAs are thought to play an important role in the norovirus entry mechanism. The non-secretor HBGAs do not add an αfucose1-2, whereas the secretor HBGAs add an αfucose1-2 contributed by α1,2fucosyltransferase enzyme (FUT2). In our study, we examined the commercially available Le^a -trisaccharide, Le^x -trisaccharide, H type 2 (disaccharide and trisaccharide), Le^b -tetrasaccharide, Le^y -tetrasaccharide, A-trisaccharide, and B-trisaccharide.

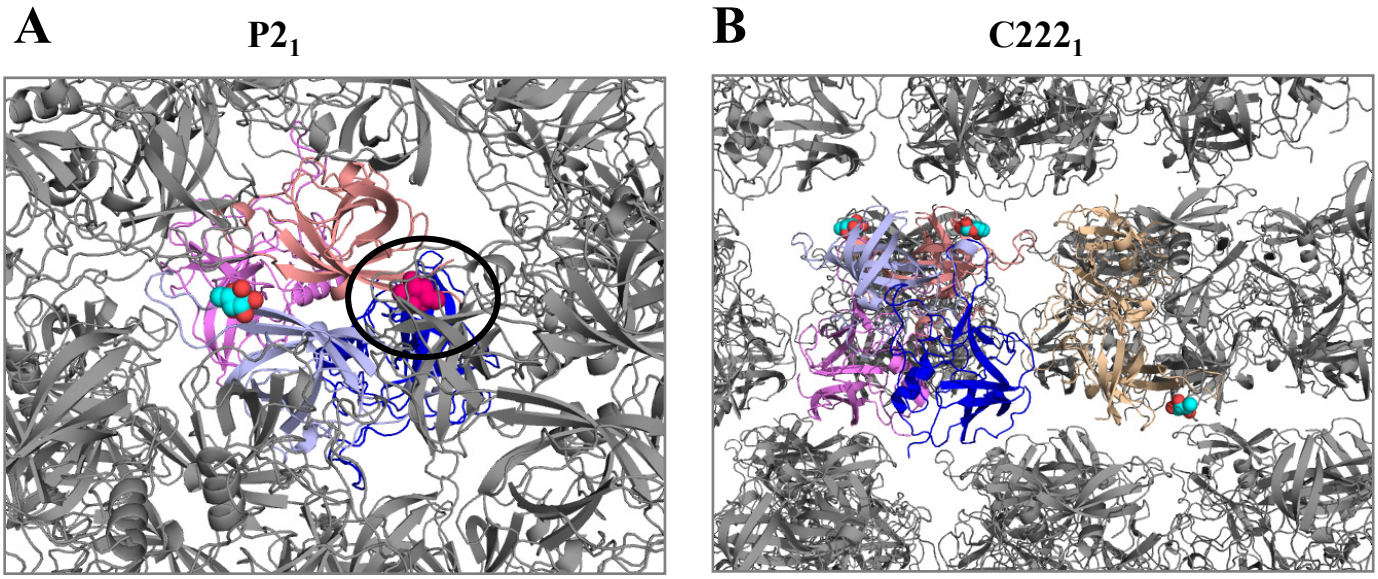

Figure S3. Crystal lattice contacts for the two different GII.10 space groups. Close neighboring P domain molecules were thought to block a second HBGA molecule from binding at the alternative HBGA binding site. (A) Shown as a top view for the $P2_1$ space group (H type 2 trisaccharide), there was only one HBGA molecule per dimer, shown as cyan/red spheres. The black circle showed the clash of the neighboring molecule that likely inhibited the second HBGA molecule (modeled in as red spheres) from binding on the dimer, compared to the "open" space for the single-bound HBGA on the left side. (B) Shown as a side view for the $C222_1$ space group (Le^b tetrasaccharide), there were two HBGAs per dimer (cyan/red spheres), as the "open" space likely allowed for the second HBGA molecule to bind to the dimer.

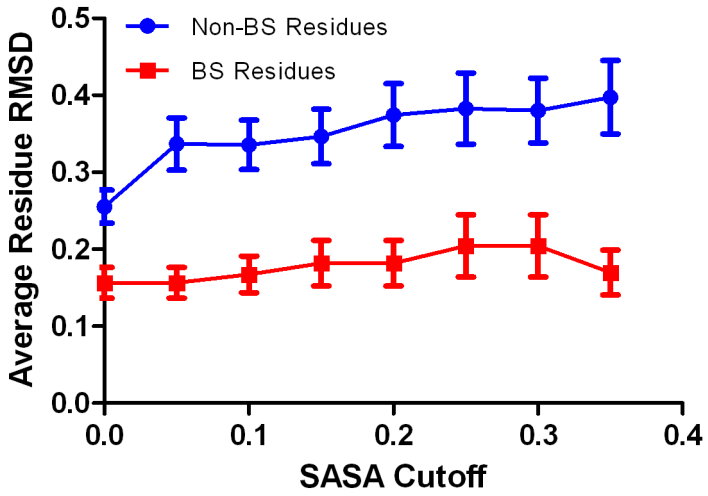

Figure S4. RMSD analysis of GII.10 bound to different HBGAs. Residues interacting with different HBGAs were structurally conserved. Average residue RMSD for HBGA binding site residues (red) and non-binding site residues (blue) within the six bound GII.10 structures. For each residue, the average RMSD observed among all pairs of structures was obtained. Using different cutoffs for relative residue solvent accessibility (SASA), the average RMSD among all binding site residues with relative SASA greater than the cutoff was plotted. Using the same SASA cutoffs, the average RMSD for non-binding site residues was plotted analogously. For all cutoffs, binding site residues were more conserved structurally as opposed to non-binding site residues, though the average RMSD values were generally low for either set of residues.

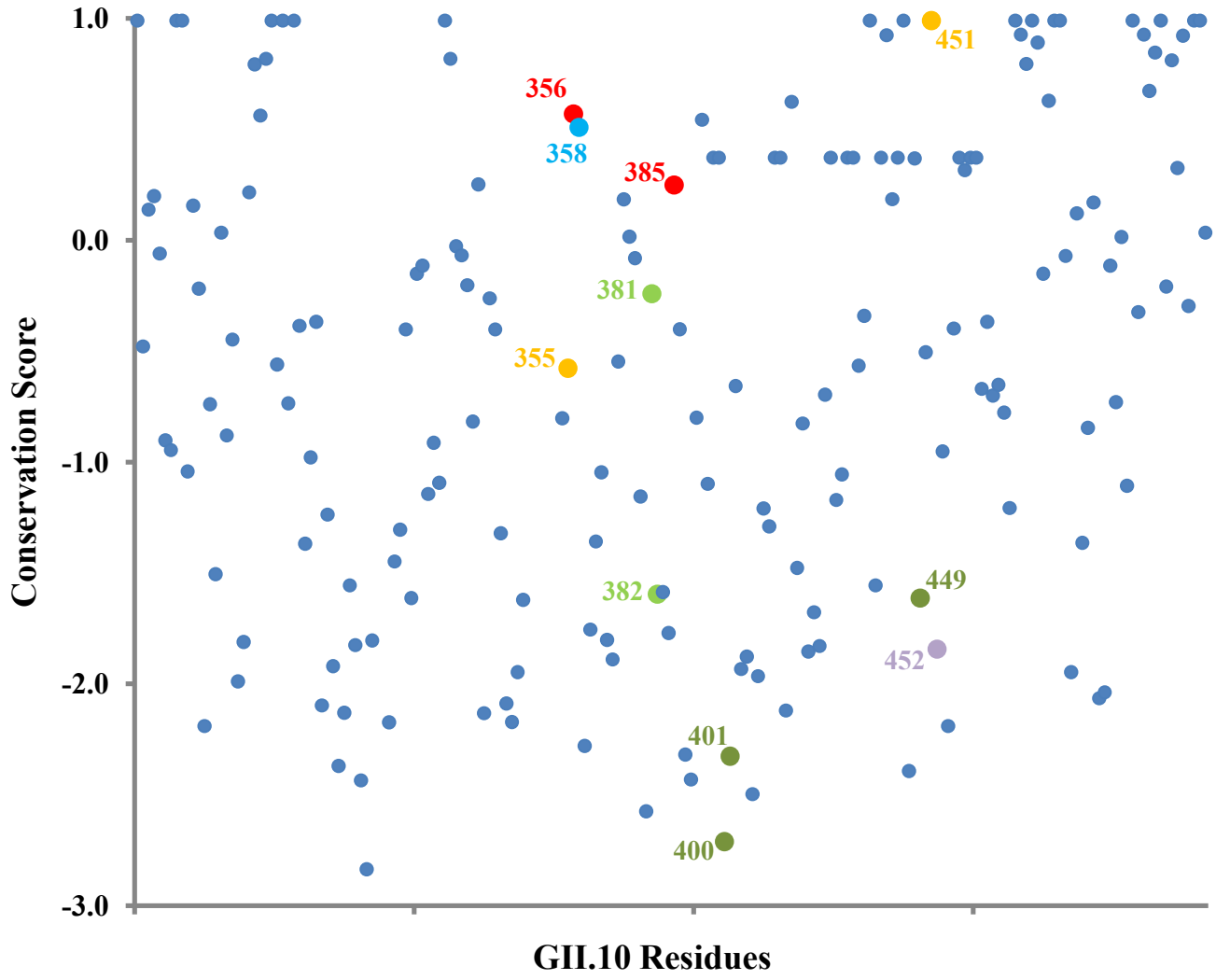

Figure S5. Residue conservation of GII.10 P domain residues. The binding of different HBGAs is likely to be associated with the conservation of surface residues. Residues observed to make binding interactions with HBGAs are labeled and colored as in figure 1SB, i.e., red (side-chain interactions with αfucose1-2), orange (backbone interactions with αfucose1-2), purple (hydrophobic interactions with αfucose1-2), light green (side-chain non-αfucose1-2 interactions), and dark green (backbone non-αfucose1-2 interactions). Residues interacting with αfucose1-2 were generally more conserved than non-αfucose1-2-interacting residues, with the exception of Tyr452, which was observed to contribute hydrophobic interactions. Shown are only residues with a relative SASA greater than the lowest relative SASA value of a binding site residue (≈0.05, Asn355).

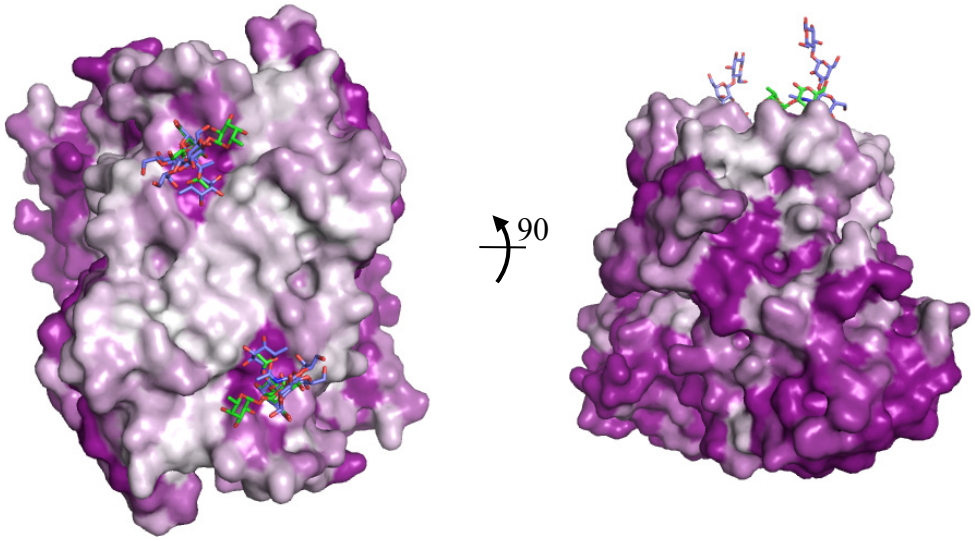

Figure S6. Surface representations of GI amino acid conservation. GI HBGA binding site appeared to be more conserved than other areas on the top of the capsid. An alignment of GI genotypes were used to determine the conservation and variability of amino acids on the GI.1 (PDB id: 2ZL5) P domain structure. As with GII, the outer-facing surface was substantially less conserved, with two major surface patches of conserved residues overlapping the HBGA binding site. The color-coded conservation ranged from a deep purple represented highly conserved amino acids to white represented highly variable.

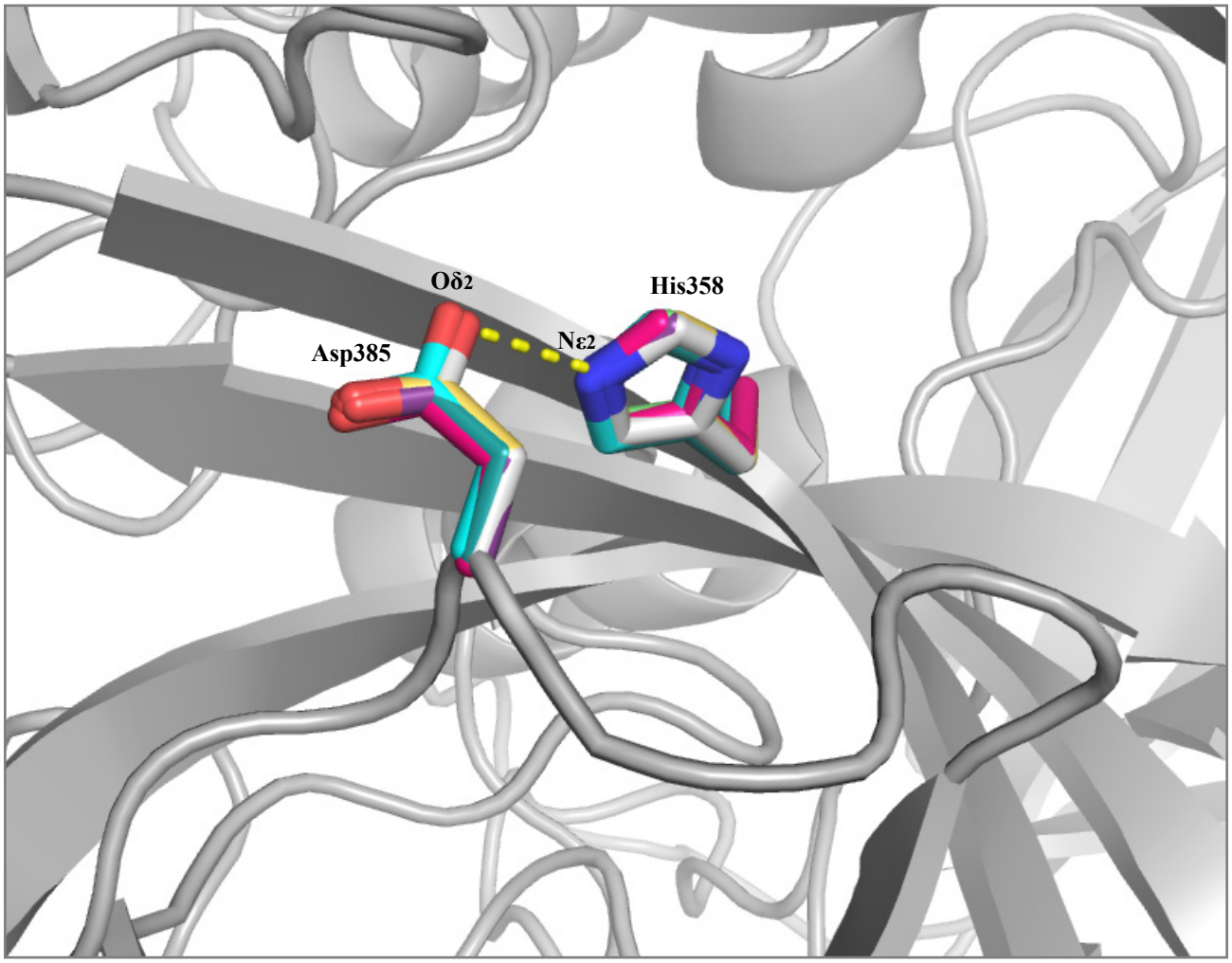

Figure S7. Potential hydrogen-bonding interaction between His358 and Asp385. Indirect residue interactions may assist the binding of HBGAs. The side-chains of the two residues in the seven GII.10 structures (apo and six holo) were overlayed on a cartoon representation of the apo structure. In the seven structures, the hydrogen-bonding interaction distance (dotted yellow line) between $N_{\varepsilon 2}$ of His358 and $O_{\delta 2}$ of Asp385 was 2.8-3.0 Å. An analogous interaction (His347 and Asp374, VA387 numbering) was observed in previously-published GII.4 structures (4), suggesting a likely indirect significance of His358 for stabilization of GII-HBGA interactions. Due to its solvent exposure and adjacency to the fucose-binding site residues, it may be possible for His358 to also participate in direct binding interactions with some HBGAs.